Hybrid-mixed stress models to the physically non-linear analysis of concrete three-dimensional structures

Carla Susana Ribeiro Garrido

Keywords: Finite Elements, Hybrid-Mixed Stress Formulations, Continuum Damage Mechanics, Legendre Polynomials, Concrete Three-dimensional Structures

Abstract: This paper presents a hybrid-mixed stress model applied to the physically nonlinear analysis of concrete three-dimensional structures. The nonlinear behaviour of concrete is modelled using Continuum Damage Mechanics. Two isotropic and elastic damage models with scalar variables have been adopted associated with a regularization technique known as nonlocal integral model. In the implementation of the model, the effective stress and displacement fields in the domain and displacements on the static boundary, which include the boundaries between elements, are independently approximated. Orthonormal Legendre polynomials are used as approximation functions. The validation of the model and its efficiency are assessed by analyzing three-dimensional problem for which known experimental and numerical results exist in the literature.

To submit to The Tenth International Conference on Computational Structures Technology, Valencia 11-14 September 2010

1. Introduction

In general, the models developed in the analysis of concrete structures are based on elasticity and plasticity classical theories. However, the cracking behaviour of the material is not properly modelled using this type of constitutive relations. The nonlinear response of concrete structures arise as a result of a series of irreversible processes that occur at the microstructure, some associated with the formation, evolution and coalescence of microcracks that are the initial damage. As the load progresses, the onset and progression of damage influence the mechanical properties of concrete, including strength and stiffness. Thus, the physically nonlinear constitutive models reflect a more realistic description of the structural behaviour of concrete elements.

With a Continuous Damage Mechanics model it is possible to analyze the evolution of the mechanical properties of a solid structural material in a localized area of the structure with large strains. These constitutive models allows the description of the properties of quasi-brittle materials experimentally verified, such as the softening behaviour, the degradation of elastic stiffness, the anisotropy and the appearance of plastic deformations [Silva, 2006]. In this work, it was adopted an isotropic damage model with one variable damage [Comi and Perego, 2001] and another one with two dependent damage variables [Mazars, 1984]. These models do not consider permanent deformations.

The mesh dependency and strain localization in zones of zero volume which was observed in models with softening and local damage analysis are overcome by using a regularization method known as nonlocal integral model, in which the spatial weighting is achieved by introducing a characteristic length. In the damage model by [Comi and Perego, 2001] the regularization is implemented considering the strain energy rate, while in the damage model of [Mazars, 1984] it is considered an equivalent strain.

This communication presents a hybrid-mixed stress formulation (HMS), in which both the stress and the displacement fields are simultaneously and independently approximated in the domain of each element. The displacements on the static boundary, which is considered to include the boundaries between elements, is also independently modelled. None of the fundamental relations is locally enforced. The compatibility conditions in the domain and the equilibrium conditions on the static boundary are enforced on average. Then, the compatibility equation is integrated by parts. The connection between elements is ensured by imposing that adjacent elements share the same boundary displacement approximation. The special interest in using HMS models is due to the possibility of obtaining locally quasi-equilibrated solutions [Almeida, 1991], which it is very convenient for structural design purposes. The use of HMS models enables also the use of a wide range of approximation functions embodying interesting properties that make very attractive their application in the solution of computational mechanics problems.

Similarly to that presented in [Silva, 2006], the stress approximation is replaced by an independent effective stress approach. Complete sets of orthonormal Legendre polynomials are used to define all the required approximations. The orthonormality property of these polynomials enables the

construction of analytical solutions for the integrations involved in the definition of the linear operators present in the governing system, which minimizes processing times and ensure high accuracy in the computations [Pereira and Freitas, 2000]. With the development of damage, the governing system becomes nonlinear and its resolution leads to the adoption of an incremental and iterative process. The iterative method used is a modified version of the Newton-Raphson technique [Zienkiewicz and Taylor, 1991b], which uses the secant matrix in the computation of the increments of all generalized variables in each stage of the iterative process.

A set of example tests is presented to illustrate the modelling of the cracking behaviour by the damage models considered in this work.

This communication is organized as follows: Section 2 describes the general formulation of the problem. Section 3 presents the damage models and the regularization method adopted. Section 4 presents the non-conventional formulation used and Section 5 discusses the most important aspects associated with the numerical implementation. The numerical tests are presented and discussed in Section 6 and Section 7 presents the main conclusions of this work and identifies possible future developments.

2. Fundamental Relations

The structural analysis requires the definition of the physical quantities involved in the description of the structural behaviour, displacements, strains, stresses and applied loads, and the equations relating those quantities, equilibrium, compatibility and constitutive relations.

Consider a body defined by its domain V, limited by the boundary Γ and referred to a Cartesian co-ordinate system. Vector $\boldsymbol{b}$ collects the components of the body force field. The static boundary Γ_σ is characterized as the region where external forces are prescribed, with components listed in the vector $\boldsymbol{t}_\gamma$. The kinematic boundary Γ_u is defined as the region where the components of the displacement field are prescribed, with components listed in the vector $\bar{\boldsymbol{u}}$. The boundary Γ is given by $\Gamma_\sigma \cup \Gamma_u$.

2.1 Equilibrium conditions

The equilibrium equations in the domain V and on the static boundary Γ_σ may be written as follows [Timoshenko and Goodier, 1970]:

$$\boldsymbol{D\sigma} + \boldsymbol{b} = \boldsymbol{0} \quad \text{in } V, \tag{1}$$

$$\boldsymbol{N\sigma} = \boldsymbol{t}_\gamma \quad \text{on } \Gamma_\sigma, \tag{2}$$

where $\boldsymbol{D}$ represents the differential equilibrium operator and $\boldsymbol{N}$ the matrix that lists the components of the unit vector normal to the static boundary. The vector $\boldsymbol{\sigma}$ collects the independent components of stress tensor and the vector $\boldsymbol{b}$ lists the components of the body forces.

2.2 Compatibility conditions

Assuming the validity of the geometric linearity hypothesis, the compatibility conditions may be written as follows [Timoshenko and Goodier, 1970]:

$$\boldsymbol{\varepsilon} = \boldsymbol{D}^{*}\,\boldsymbol{u} \qquad \text{in } V, \tag{3}$$

$$\boldsymbol{u} = \overline{\boldsymbol{u}} \qquad \text{on } \Gamma_u. \tag{4}$$

Vectors $\boldsymbol{\varepsilon}$ and $\boldsymbol{u}$ lists the independent components of the strain tensor and the displacement field components, respectively. The matrix $\boldsymbol{D}^{*}$ corresponds to the differential compatibility operator, where $\boldsymbol{D}$ and $\boldsymbol{D}^{*}$ are adjoint, namely:

$$\boldsymbol{D}^{*}_{ij} = (-1)^{n+1}\boldsymbol{D}_{ji} \tag{5}$$

being n the order of differential operator and $\boldsymbol{D}^{*}_{ij} = \boldsymbol{D}_{ji}$ when n =1.

2.3 Constitutive relation

Assuming an elastic and nonlinear behaviour to the concrete, the vector that lists the components of the stress tensor, $\boldsymbol{\sigma}$, and the vector that lists the components of the strain tensor, $\boldsymbol{\varepsilon}$, are related as follows:

$$\boldsymbol{\sigma} = \widetilde{\boldsymbol{K}} : \boldsymbol{\varepsilon}. \tag{6}$$

The above equation, written in the stiffness format, may be rewritten in the flexibility format:

$$\boldsymbol{\varepsilon} = \widetilde{\boldsymbol{F}} : \boldsymbol{\sigma}. \tag{7}$$

The operator $\widetilde{\boldsymbol{K}}\{\widetilde{\boldsymbol{F}}\}$ is the constitutive stiffness {flexibility} tensor of the material whit a nonlinear behaviour. In the case of linear elastic behaviour of the material, the tensor $\widetilde{\boldsymbol{K}}\{\widetilde{\boldsymbol{F}}\}$ is equal to the constitutive stiffness {flexibility} tensor of linear elastic material $\boldsymbol{K}\{\boldsymbol{F}\}$.

3. Damage Models

The nonlinear behaviour of concrete is described using two alternative isotropic damage models, both with evolution laws depending on the actual strain tensor components.

On isotropic damage models, the constitutive relation usually involves the strain equivalence principle proposed by [Lemaitre and Chaboche, 1988], which states that the deformation of the non damaged space where the effective stress acts is the same at the damaged space, ie, $\tilde{\varepsilon} = \varepsilon$.

For multiaxial damage models, it is considered an equivalent strain, $\tilde{\varepsilon}$, which may be simply defined by [Lemaitre, 1992]:

$$\widetilde{\varepsilon} = Y = \frac{1}{2}\,\boldsymbol{\varepsilon} : \boldsymbol{K} : \boldsymbol{\varepsilon}. \tag{8}$$

Considering the strain equivalence principle, the variable Y represents the elastic strain energy rate, ie, the free energy range, ψ, following the increase of the damage variable d, to constant deformation and temperature [Lemaitre, 1992].

However, the above definition leads to the same traction and compression behaviour. To solve this situation, it is necessary to adopt other formulations that reflect more accurately the realistic concrete behaviour.

3.1 Damage model by [Comi and Perego, 2001]

The damage model with only a scalar damage variable, d, introduced by [Comi and Perego, 2001], is based on the Helmholtz free energy density, defined as:

$$\psi = \frac{1}{2}(1-d)\,\boldsymbol{\varepsilon} : \boldsymbol{K} : \boldsymbol{\varepsilon} + \psi_{in}(\xi), \quad \text{with } d \in [0,1[. \tag{9}$$

The function $\psi_{in}(\xi)$ represents the inelastic energy density, expressed in terms of an internal scalar variable of kinematic nature, ξ. For the expression (9), [Comi and Perego, 2001] define the following state equations:

$$\boldsymbol{\sigma} = \frac{\partial \psi}{\partial \boldsymbol{\varepsilon}} = (1-d)\,\boldsymbol{K} : \boldsymbol{\varepsilon}, \tag{10}$$

$$Y = -\frac{\partial \psi}{\partial d} = \frac{1}{2}\boldsymbol{\varepsilon} : \boldsymbol{K} : \boldsymbol{\varepsilon}, \tag{11}$$

$$\chi = \frac{\partial \psi}{\partial \xi} = \psi'_{in}(\xi) = k \ln^n\left(\frac{c}{1-\xi}\right). \tag{12}$$

The state variables are the elastic strain, $\boldsymbol{\varepsilon}$, the damage variable, d, and the internal variable, ξ. Their associated variables are the stress, $\boldsymbol{\sigma}$, the elastic strain energy rate, Y, and the thermodynamic force, χ. The parameters n, k and c depend on the material. The potential of dissipation is defined as:

$$f(Y-\chi) = Y - \chi = \frac{1}{2}\boldsymbol{\varepsilon} : \boldsymbol{K} : \boldsymbol{\varepsilon} - \chi \leq 0. \tag{13}$$

Thus, the equivalent strain becomes equal to the elastic strain energy rate, Y. The evolution laws for the internal variables are obtained from the potential of dissipation defined above:

$$\dot{d} = \frac{\partial f}{\partial Y}\dot{\gamma} = \dot{\gamma}, \tag{14}$$

$$\dot{\xi} = -\frac{\partial f}{\partial \chi}\dot{\gamma} = \dot{\gamma}, \tag{15}$$

where γ is a positive scalar. According to equations (14) and (15), it is possible to verify that in this constitutive model, the damage variable, d, the internal variable, ξ, and the positive scalar, γ, take the same value.

The Kuhn-Tucker loading-unloading conditions are defined by:

$$f \leq 0, \quad \dot{\gamma} \geq 0, \quad \dot{\gamma} f = 0. \tag{16}$$

The potential of dissipation may be rewritten as a function of the effective stress, $\boldsymbol{\sigma} = \tilde{\boldsymbol{\sigma}}(1-d)$, and the elastic flexibility matrix $\boldsymbol{F}$ of the virgin material, such as:

$$f(Y-\chi) = Y - \chi = \frac{1}{2}\tilde{\boldsymbol{\sigma}} : \boldsymbol{F} : \tilde{\boldsymbol{\sigma}} - \chi. \tag{17}$$

Despite the damage model presented in this section consider a similar concrete behaviour for traction and compression solicitations, this model is adequate for study structures subjected mainly to traction efforts. In this work, it is considered that there is damage only if tr$\boldsymbol{\varepsilon} \geq 0$.

3.2 Damage model by [Mazars, 1984]

The damage model originally developed by [Mazars, 1984] models the physically nonlinear concrete behaviour by introducing a scalar damage variable and assuming that the onset and evolution of damage results merely from the occurrence of positive extensions. Thus, the equivalent strain is calculated considering only the positive part of the principal components of the strain tensor and may be defined such as:

$$\tilde{\varepsilon} = \|\langle \boldsymbol{\varepsilon} \rangle\| = \sqrt{\langle \varepsilon_{\mathrm{I}} \rangle_+^2 + \langle \varepsilon_{\mathrm{II}} \rangle_+^2 + \langle \varepsilon_{\mathrm{III}} \rangle_+^2} = \sqrt{\sum_{i=I}^{i=III} \langle \varepsilon_i \rangle_+^2} \tag{18}$$

being ε_i the principal strains. The i-ith positive component of the principal strain tensor is given by:

$$\langle (\varepsilon_{\mathrm{i}}) \rangle_+ = \frac{1}{2} \left[(\varepsilon_{\mathrm{i}}) + |(\varepsilon_{\mathrm{i}})| \right] \tag{19}$$

According to this constitutive model, material has a linear elastic behaviour until the threshold ε_{d0} is reached. From this point on, material becomes damaged and presents a non-linear behaviour. In one-dimensional case, the parameter value ε_{d0} is determined by the maximum strength value in an uniaxial tension tests, f_t, given by:

$$\varepsilon_{d0} = \frac{f_t}{E} \tag{20}$$

The potential of dissipation is defined as:

$$f(\tilde{\varepsilon}, d) = \tilde{\varepsilon} - \chi(d) \leq 0 \tag{21}$$

with
$$\chi(d) = \varepsilon_{d0}, \qquad d = 0$$
$$\chi(d) = \max \{\max [\varepsilon\ (d)], \varepsilon_{d0}\}, \qquad d > 0$$

Assuming the irreversibility of the damage process, the evolution law of the variable d is equivalent to:

$$\dot{d} = 0 \text{ if } f < 0 \text{ or } f = 0 \text{ and } \dot{f} < 0\,, \tag{22}$$

$$\dot{d} = \mathbf{F}(\tilde{\varepsilon})\, \langle \dot{\tilde{\varepsilon}} \rangle_+ \text{ if } f = 0 \text{ and } \dot{f} = 0\,, \tag{23}$$

where $\mathbf{F}(\tilde{\varepsilon})$ is a continuous and positive equivalent strain function. Then, $\dot{d} \geq 0$ for any $\dot{\tilde{\varepsilon}} \geq 0$.

For traction and compression uniaxial cases, two independent scalar variables, d_t and d_c, are defined which represent the traction and compression damage, respectively. The evolution laws for these two variables are given by:

$$\dot{d}_t = \mathbf{F}_t(\tilde{\varepsilon})\, \langle \dot{\tilde{\varepsilon}} \rangle_+ \tag{24}$$

$$\dot{d}_c = \mathbf{F}_c(\tilde{\varepsilon})\, \langle \dot{\tilde{\varepsilon}} \rangle_+ \tag{25}$$

where:

$$\mathbf{F}_t(\tilde{\varepsilon}) = \frac{\varepsilon_{d0}(1 - A_t)}{\tilde{\varepsilon}^2} + \frac{A_t\, B_t}{\exp\left[B_t(\tilde{\varepsilon} - \varepsilon_{d0})\right]} \tag{26}$$

$$\mathbf{F}_c(\tilde{\varepsilon}) = \frac{\varepsilon_{d0}(1 - A_c)}{\tilde{\varepsilon}^2} + \frac{A_c\, B_c}{\exp[B_c(\tilde{\varepsilon} - \varepsilon_{d0})]}. \tag{27}$$

The parameters A_t, B_t, ε_{d0}, A_c and B_c are the material characteristic parameters. The first three may be determined trough traction uniaxial tests with controlled strain and the latter two trough compression traction uniaxial tests with controlled strain, too.

Integrating expressions (24) and (25) we obtain:

$$d_t(\tilde{\varepsilon}) = 1 - \frac{\varepsilon_{d0}(1 - A_t)}{\tilde{\varepsilon}} - \frac{A_t}{\exp\left[B_t(\tilde{\varepsilon} - \varepsilon_{d0})\right]} \tag{28}$$

$$d_c(\tilde{\varepsilon}) = 1 - \frac{\varepsilon_{d0}(1 - A_c)}{\tilde{\varepsilon}} - \frac{A_c}{\exp\left[B_c(\tilde{\varepsilon} - \varepsilon_{d0})\right]} \tag{29}$$

The damage variable may be defined as a linear combination of d_t and d_c, to reflect more complex stress conditions. The corresponding damage variable is defined as:

$$d = \alpha_t d_t + \alpha_c d_c \tag{30}$$

with α_t + α_c = 1. Equation (30) concerns the uniaxial cases characteristics. The coefficients α_t and α_c take the unit value in traction and compression uniaxial tests, respectively. According to [Perego, 1990], these coefficients are determined as follows:

$$\alpha_t = \frac{\sum_i \langle \boldsymbol{\varepsilon}_{T_i} \rangle_+}{\sum_i \langle \boldsymbol{\varepsilon}_{T_i} \rangle_+ + \sum_i \langle \boldsymbol{\varepsilon}_{C_i} \rangle_+} \tag{31}$$

$$\alpha_c = \frac{\sum_i \langle \boldsymbol{\varepsilon}_{C_i} \rangle_+}{\sum_i \langle \boldsymbol{\varepsilon}_{T_i} \rangle_+ + \sum_i \langle \boldsymbol{\varepsilon}_{C_i} \rangle_+} \tag{32}$$

and

$$\varepsilon_T = \frac{1 + \upsilon}{E} \langle \tilde{\boldsymbol{\sigma}} \rangle_+ - \frac{\upsilon}{E} \sum_i \langle \tilde{\boldsymbol{\sigma}}_i \rangle_+ \mathbf{I}; \tag{33}$$

$$\varepsilon_C = \frac{1 + \upsilon}{E} \langle \tilde{\boldsymbol{\sigma}} \rangle_- - \frac{\upsilon}{E} \sum_i \langle \tilde{\boldsymbol{\sigma}}_i \rangle_- \mathbf{I}; \tag{34}$$

where $\mathbf{I}$ denote the tensor identity and $\langle \tilde{\boldsymbol{\sigma}} \rangle_+$ and $\langle \tilde{\boldsymbol{\sigma}} \rangle_-$ represent, respectively, the positive and negative parts of the principal effective stress tensor, which is calculated according to the current strains by applying the elastic isotropic relation.

3.3 Regularization technique

In quasi-brittle materials, such as concrete, the localization of the strains evolution occurs on a restrict material band. The finite element formulation based on a local constitutive model is unable to reproduce the real concrete behaviour because, at the limit of a refinement procedure, the model response is achieved with zero energy dissipation. This problem may be overcome by using regularization methods. In this work, it is adopted a model known as nonlocal integral model in which the constitutive relation at a given point depends on the values that some physical quantities present at neighbouring points [Bazant, 1992].

So, it is introduced a non-local variable, $\bar{A}$, on the secant constitutive relation or on the potential of dissipation, f. The non-local variable, $\bar{A}$, is obtained through a weighing like the one defined in [Mazars et al, 1991; Bazant, 1992; Pijaudier-Cabot et al., 1994]:

$$\bar{A}(x) = \int_V W(x, s)\, A(s)\, ds, \tag{35}$$

where V is the domain structure and $W(x,s)$ is the weighting function, usually taken as the standard Gaussian function defined as:

$$W(x,s) = \frac{1}{W_0(x)} \exp\left(-\frac{\|x-s\|^2}{2l^2}\right) \tag{36}$$

$$\text{with} \qquad W_0(x) = \int_V \exp\left(-\frac{\|x-s\|^2}{2l^2}\right) ds. \tag{37}$$

In the damage model by [Mazars, 1984], the regularization trough the non local method is implemented considering the equivalent strain value, $\tilde{\varepsilon}$, while in the damage model by [Comi and Perego, 2001] that implementation is based on the strain energy rate value, $\bar{Y}$.

4. Hybrid-mixed stress model

The approximations required by the hybrid-mixed stress model can be expressed in the following format:

$$\tilde{\boldsymbol{\sigma}} = \boldsymbol{S}_v \tilde{\boldsymbol{X}} \qquad \text{in } V\,, \tag{38}$$

$$\boldsymbol{u} = \boldsymbol{U}_v \boldsymbol{q}_v \qquad \text{in } V, \tag{39}$$

$$\boldsymbol{u} = \boldsymbol{U}_\gamma \boldsymbol{q}_\gamma \qquad \text{on } \Gamma_\sigma, \tag{40}$$

The vector $\tilde{\boldsymbol{\sigma}}$ lists the independent components of the effective stress tensor and the vector $\boldsymbol{u}$ lists the components of the displacement field. Matrices $\boldsymbol{S}_v$, $\boldsymbol{U}_v$ and $\boldsymbol{U}_\gamma$ collect their approximation functions and the vectors $\tilde{\boldsymbol{X}}$, $\boldsymbol{q}_v$ and $\boldsymbol{q}_\gamma$ list the associated weights (generalized variables).

The generalized strains components,$\mathbf{e}$, the generalized forces in domain,$\boldsymbol{Q}_v$, and the generalized forces at the static boundary, $\boldsymbol{Q}_\gamma$, may be obtained through the following definitions:

$$\mathbf{e} = \int_V \boldsymbol{S}_v{}^T \boldsymbol{\varepsilon}\, \mathrm{dV}\,. \tag{41}$$

$$\mathbf{Q}_v = \int_V \boldsymbol{U}_v{}^T \boldsymbol{b}\, \mathrm{dV}. \tag{42}$$

$$\mathbf{Q}_\gamma = \int_{\Gamma_\sigma} \boldsymbol{U}_\gamma^T \boldsymbol{t}_\gamma \mathrm{d}\Gamma_\sigma. \tag{43}$$

The elementary governing system is obtained by enforcing on average, in a weighted residual form, the fundamental conditions. For this purpose it is necessary to rewrite the fundamental relations on the basis of known quantities. The tension field in each point, $\boldsymbol{\sigma}$, is determined based on the effective stress field, $\tilde{\boldsymbol{\sigma}}$, through the use of equation:

$$\boldsymbol{\sigma} = (\mathbf{I} - \boldsymbol{\Omega})\, \tilde{\boldsymbol{\sigma}} \tag{44}$$

where $\boldsymbol{\Omega}$ is the matrix representation of the fourth-order damage tensor and $\mathbf{I}$ represents the identity matrix.

In order to obtain a general formulation, the stress-effective stress relation will be considered in the format shown in Equation (44). So, the fundamental relations enforced on average may be written as follows:

Equilibrium in V; $$\int_{\mathrm{V}} \boldsymbol{U}_v^T\{\boldsymbol{D}[(\mathbf{I}-\boldsymbol{\Omega})\widetilde{\boldsymbol{\sigma}}]+\boldsymbol{b}\}\mathrm{dV}=0 \tag{45}$$

Equilibrium on Γ_σ; $$\int_{\Gamma_\sigma} \boldsymbol{U}_\gamma^T\{\boldsymbol{N}[(\mathbf{I}-\boldsymbol{\Omega})\widetilde{\boldsymbol{\sigma}}]-\boldsymbol{t}_\gamma\}\,\mathrm{d}\Gamma_\sigma=0 \tag{46}$$

Constitutive relation in V; $$\int_{\mathrm{V}} \boldsymbol{S}_v{}^T\left(\boldsymbol{\varepsilon}-\boldsymbol{F}\boldsymbol{S}_v\widetilde{\boldsymbol{X}}\right)\mathrm{dV}=0 \tag{47}$$

Compatibility in V. $$\int_{\mathrm{V}} \boldsymbol{S}_v{}^T(\boldsymbol{\varepsilon}-\boldsymbol{D}^*\boldsymbol{u})\mathrm{dV}=0 \tag{48}$$

The equations above may be rewritten in the following format:

Equilibrium in V; $$\int_{\mathrm{V}} \boldsymbol{U}_v^T(\boldsymbol{D}\boldsymbol{S}_v)\mathrm{dV}\,\widetilde{\boldsymbol{X}}-\int_{\mathrm{V}} \boldsymbol{U}_v^T[\boldsymbol{D}(\boldsymbol{\Omega}\boldsymbol{S}_v)]\mathrm{dV}\,\widetilde{\boldsymbol{X}}=-\int_{\mathrm{V}} \boldsymbol{U}_v^T\boldsymbol{b}\mathrm{dV} \tag{49}$$

Equilibrium on Γ_σ; $$\int_{\Gamma_\sigma} \boldsymbol{U}_\gamma^T(\boldsymbol{N}\boldsymbol{S}_v)\mathrm{d}\Gamma_\sigma\,\widetilde{\boldsymbol{X}}-\int_{\Gamma_\sigma} \boldsymbol{U}_\gamma^T[\boldsymbol{N}(\boldsymbol{\Omega}\boldsymbol{S}_v)]\mathrm{d}\Gamma_\sigma\,\widetilde{\boldsymbol{X}}=\int_{\Gamma_\sigma} \boldsymbol{U}_\gamma^T\boldsymbol{t}_\gamma\,\mathrm{d}\Gamma_\sigma \tag{50}$$

Constitutive relation in V; $$\int_{\mathrm{V}} \boldsymbol{S}_v{}^T\boldsymbol{\varepsilon}\,\mathrm{dV}=\int_{\mathrm{V}} \boldsymbol{S}_v{}^T\boldsymbol{F}\boldsymbol{S}_v\mathrm{dV}\widetilde{\boldsymbol{X}} \tag{51}$$

Compatibility in V. $$\int_{\mathrm{V}} \boldsymbol{S}_v{}^T\boldsymbol{\varepsilon}\,\mathrm{dV}=\int_{\mathrm{V}} \boldsymbol{S}_v{}^T\,\boldsymbol{D}^*\,\boldsymbol{u}\,\mathrm{dV} \tag{52}$$

Integrating by parts the second term of the Equation (52) to accommodate the Dirichlet condition (Equation (4)) and inserting the approximations (39) e (40) it is possible to obtain:

$$\mathbf{e}=-\int_{\mathrm{V}}(\boldsymbol{D}\boldsymbol{S}_v)^T\,\boldsymbol{U}_v\,\mathrm{dV}\,\boldsymbol{q}_v+\int_{\Gamma_\sigma}(\boldsymbol{N}\boldsymbol{S}_v)^T\boldsymbol{U}_\gamma\,\mathrm{d}\Gamma_\sigma\boldsymbol{q}_\gamma+\int_{\Gamma_u}(\boldsymbol{N}\boldsymbol{S}_v)^T\overline{\boldsymbol{u}}\,\mathrm{d}\Gamma_u \tag{53}$$

Therefore, structural operators are defined such as:

$$\mathbf{A}_v=\int_{\mathrm{V}}(\boldsymbol{D}\boldsymbol{S}_v)^T\,\boldsymbol{U}_v\,\mathrm{dV}, \tag{54}$$

$$\boldsymbol{M}_v=\int_{\mathrm{V}}\boldsymbol{U}_v^T[\boldsymbol{D}(\boldsymbol{\Omega}\boldsymbol{S}_v)]\mathrm{dV}, \tag{55}$$

$$\mathbf{A}_\gamma=\int_{\Gamma_\sigma}(\boldsymbol{N}\boldsymbol{S}_v)^T\boldsymbol{U}_\gamma\,\mathrm{d}\Gamma_\sigma, \tag{56}$$

$$\boldsymbol{M}_\gamma=\int_{\Gamma_\sigma}\boldsymbol{U}_\gamma^T[\boldsymbol{N}(\boldsymbol{\Omega}\boldsymbol{S}_v)]\mathrm{d}\Gamma_\sigma, \tag{57}$$

$$\mathbb{F}=\int_{\mathrm{V}}\boldsymbol{S}_v{}^T\boldsymbol{F}\boldsymbol{S}_v\mathrm{dV}, \tag{58}$$

$$\bar{\mathbf{e}}=\int_{\Gamma_u}(\boldsymbol{N}\boldsymbol{S}_v)^T\overline{\boldsymbol{u}}\,\mathrm{d}\Gamma_u\,. \tag{59}$$

Considering the definition given above, the fundamental relations may be written in the following matrix format:

Equilibrium in V; $(\boldsymbol{A}_v^T - \boldsymbol{M}_v)\,\widetilde{\boldsymbol{X}} = -\boldsymbol{Q}_v$ (60)

Equilibrium on Γ_σ; $(-\boldsymbol{A}_\gamma^T + \boldsymbol{M}_\gamma)\,\widetilde{\boldsymbol{X}} = -\boldsymbol{Q}_\gamma$ (61)

Constitutive relation in V; $\mathbf{e} = \mathbb{F}\widetilde{\boldsymbol{X}}$ (62)

Compatibility in V. $\mathbf{e} = -\mathbf{A}_v\boldsymbol{q}_v + \mathbf{A}_\gamma\boldsymbol{q}_\gamma + \bar{\mathbf{e}}$ (63)

Combining the conditions (62) and (63):

$$\mathbb{F}\widetilde{\boldsymbol{X}} = -\mathbf{A}_v\boldsymbol{q}_v + \mathbf{A}_\gamma\boldsymbol{q}_\gamma + \bar{\mathbf{e}} \tag{64}$$

From (60), (61) and (64), the governing system for each hybrid-mixed stress finite element may be written in matrix form:

$$\begin{bmatrix} \mathbb{F} & \mathbf{A}_v & -\mathbf{A}_\gamma \\ \boldsymbol{A}_v^T - \boldsymbol{M}_v & \mathbf{0} & \mathbf{0} \\ -\boldsymbol{A}_\gamma^T + \boldsymbol{M}_\gamma & \mathbf{0} & \mathbf{0} \end{bmatrix} \begin{bmatrix} \widetilde{\boldsymbol{X}} \\ \boldsymbol{q}_v \\ \boldsymbol{q}_\gamma \end{bmatrix} = \begin{bmatrix} \bar{\mathbf{e}} \\ -\boldsymbol{Q}_v \\ -\boldsymbol{Q}_\gamma \end{bmatrix} \tag{65}$$

In common cases of isotropic damage models, in which the relation $\boldsymbol{\sigma} = (1-d)\,\widetilde{\boldsymbol{\sigma}}$ is valid, it is possible to define the operator $\boldsymbol{M}_\gamma$ and the operator $\boldsymbol{M}_v$ is obtained integrating by parts Equation (55):

$$\boldsymbol{M}_\gamma = \int_{\Gamma_\sigma} \boldsymbol{U}_\gamma^T(\boldsymbol{N}\, d\boldsymbol{S}_v)\,\mathrm{d}\Gamma_\sigma \tag{66}$$

$$\boldsymbol{M}_v = -\int_{\mathrm{V}} (\boldsymbol{D}^*\boldsymbol{U}_v)^T d\,\boldsymbol{S}_v \mathrm{dV} + \int_{\Gamma} (\boldsymbol{N}^*\boldsymbol{U}_v)^T\, d\,\boldsymbol{S}_v \mathrm{d}\Gamma \tag{67}$$

5. Numerical Implementation

Complete sets of Legendre orthonormal polynomials are used to define all approximations required by the hybrid-mixed stress model. The use of these approximation bases leads to highly sparse governing systems. The properties of Legendre polynomials can be exploited in order to obtain closed form solutions for the integrations involved in the computation of all linear structural operators..

In the three-dimensional case, the approximation functions are of given by $P_i(\xi) \times P_j(\eta) \times P_k(\zeta)$, where $\xi, \eta, \zeta \in$ [-1.0, 1.0], and the number of approximation functions for each component is given by $(1+n_\xi)(1+n_\eta)(1+n_\zeta)$, where n_ξ, n_η and n_ζ represent the maximum degree of the approximation in ξ, η and ζ, directions, respectively. The number of rows in the matrices storing the approximation functions corresponds to the number of independent components to be approximated.

To solve the non-linear governing system, a modified version of the Newton-Raphson technique [Zienkiewicz and Taylor, 1991] is used, and a secant matrix is involved in the computation of the generalized variables increments in every stage of the iterative process.

The algorithm used to solve the nonlinear governing system at a given loading step n can be described as follows:

1. *Error* = 10 x tolerance and iter=1;
2. While *Error* > tolerance
   - $\mathbf{sol}_j$, at the beginning of the new load step, represents the vector solution obtained at the previous step. In subsequent iterations, the solution vector is updated. The independent variables listed in the solution vector correspond to the generalized quantities $\widetilde{\boldsymbol{X}}, \boldsymbol{q}_v$ and $\boldsymbol{q}_\gamma$;
   - Use the Kuhn-Tucker conditions to obtain the new values of damage variable at each integration point;
   - Determination of the residues vector $\mathbf{R}$, which is defined in iteration j +1 by:

$$\mathbf{R}_{j+1} = \begin{bmatrix} \mathbf{R_1} \\ \mathbf{R_2} \\ \mathbf{R_3} \end{bmatrix}_{j+1} = \begin{bmatrix} \mathbb{F}\widetilde{\boldsymbol{X}}_j + \boldsymbol{A}_v \boldsymbol{q}_{vj} - \boldsymbol{A}_\gamma \boldsymbol{q}_{\gamma j} - \bar{\mathbf{e}} \\ (\boldsymbol{A}_v^T - \boldsymbol{M}_v)_j \widetilde{\boldsymbol{X}}_j + \boldsymbol{Q}_v \\ (-\boldsymbol{A}_\gamma^T + \boldsymbol{M}_\gamma)_j \widetilde{\boldsymbol{X}}_j + \boldsymbol{Q}_\gamma \end{bmatrix} \tag{68}$$

   - Update the variable *Error*, assuming *Error* = $\frac{\|\mathbf{R}\|}{C}$, where C is a normalization constant;
   - Determination of the evolution of the solution vector:

$$\mathbf{A}_j \boldsymbol{\Delta sol} = -\mathbf{R}_{j+1}, \tag{69}$$

     where $\mathbf{A}$ represents the secant matrix of the governing global system:

$$\begin{bmatrix} \mathbb{F} & \mathbf{A}_v & -\mathbf{A}_\gamma \\ \boldsymbol{A}_v^T - \boldsymbol{M}_v & \mathbf{0} & \mathbf{0} \\ -\boldsymbol{A}_\gamma^T + \boldsymbol{M}_\gamma & \mathbf{0} & \mathbf{0} \end{bmatrix}_j \begin{bmatrix} \Delta\widetilde{\boldsymbol{X}} \\ \Delta \boldsymbol{q}_v \\ \Delta \boldsymbol{q}_\gamma \end{bmatrix} = - \begin{bmatrix} \mathbf{R_1} \\ \mathbf{R_2} \\ \mathbf{R_3} \end{bmatrix}_{j+1} \tag{70}$$

   - Calculation of the new solution vector: $\mathbf{sol}_{j+1} = \mathbf{sol}_j + \boldsymbol{\Delta sol}$;
   - Update the non-local quantity at each integration point using the weighting function defined in expression (35).
   - iter = iter + 1.
3. Storage solution for the load step $(n+1)$ and go to the next increment.

It is necessary to establish an appropriate relation between the degrees of the approximation functions, such as: n_{U_v} = n_{S_v}-1 and n_{U_γ}= n_{U_v}-1, to avoid spurious modes and to ensure an adequate conditioning for the governing system.

6. Results

The following numerical examples illustrate the use of the hybrid-mixed stress model associated with two isotropic and elastic damage models, namely, the model presented by [Comi and Perego, 2001] and the model introduced by [Mazars, 2001]. The analysis of a fixed-fixed beam under a uniform load enables to assess the ability and performance of these models to describe the cracking behaviour of the concrete structures. The second one is an L-shaped structure with a prescribed displacement that shows the localization of stresses at the singular zone.

The values of the material parameters of the model presented by [Comi and Perego, 2001] are n =12, K = 5,8×10^{-14}MPa and c = 405 and for the damage model of [Mazars, 1984] the following values are considered: A_t = 0.3, B_t = 8000, ε_{d0} = 9.34×10^{-5}, A_c = 0.85 and B_c = 1050. For both examples, these model parameters are considered and the elastic concrete parameters adopted are: E = 29.2GPa and υ = 0.2. The characteristic length, l, is equal to 0.2m in the first example, while in the second one is equal to 0.1m.

6.1 Example 1: fixed-fixed beam

A fixed-fixed beam with 10 meters of length is analysed. Its cross section has dimensions 2mx2m and the structure is under an uniform distributed load equal to 0.75MPa, as ilustrated in Figure (1). A mesh with five finite elements is adopted and each one corresponds to a cube characterized by an edge's length equal to 2m. The degress of the aproximation functions are n_{S_v} = 5, n_{U_v} = 4 and n_{U_γ} = 3, which corresponds to 9507 degrees of freedom. The numerical results are obtained by considering a mesh of (20x20x20) Lobatto integration points.

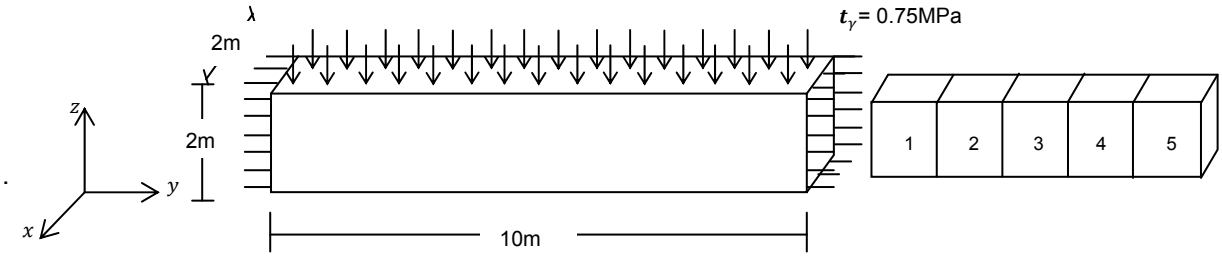

Figure 1 – Example 1: Definition of the geometry, the load case and the finite elements mesh.

Actually, this structure is not classified as a beam due to its geometry. However, it enables a qualitative comparison between the numerical results obtained and the known results for a fixed-fixed beam under a distributed uniform load in all the spam. The stress diagrams $\sigma_{yy}\{\tilde{\sigma}_{yy}\}$ and $\sigma_{yz}\{\tilde{\sigma}_{yz}\}$ are related, respectively, with the diagrams of the bending moment and the shear force in linear {non-linear} regime. The stresses diagrams and damage distribution presented occur on a plane of equation x=1m.

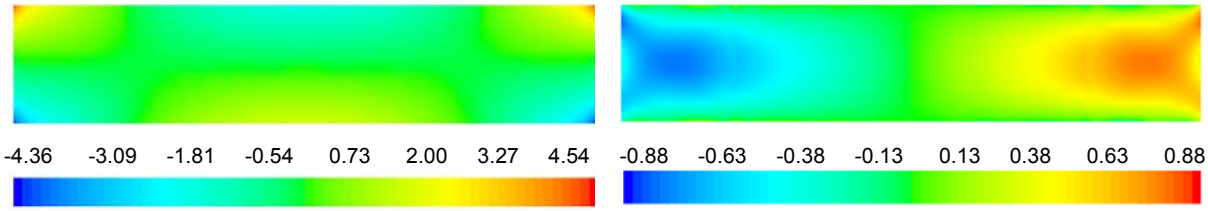

(a) σ_{yy} (MPa) (b) σ_{yz} (MPa)

Figure 2 – Example 1: stress distribution in linear regime for t_γ= 0.25MPa (plane x=1.0m).

Stress diagrams in linear regime for a load t_γ=0.25MPa are presented. The highest value of the tensile and the compression stress (Figure 2.a) is related, respectively, to the negative bending moment at the fixed sections and to the positive moment at the middle-spam. The stress distribution

σ_{yz} has a null value in the section at the midd-spam (Figure 2.b), which corresponds to the null point on the shear force diagram. Therefore, the results obtained in elastic regime reproduce the numerical results of the literature.

The bending efforts cause, essentially, tensile stresses of the top fibers at the fixed sections and bottom fibers at mid-spam zone. However, as expected, the beginning of the damaging process occurs on the first ones due to the highest tensile stresses. Therefore, the decreasing of strength and stiffness at those zones leads to the collapse of the structure.

The effective stress distribution is very similar in both damage models considered in this analysis. So, only the stress distribution in nonlinear regime by the damage model of [Mazars, 1984] for t_γ= 0.75MPa is illustrated and the maximum and minimum values of effective stresses obtained by the damage model by [Comi and Perego, 2001] are presented at the Table (1).

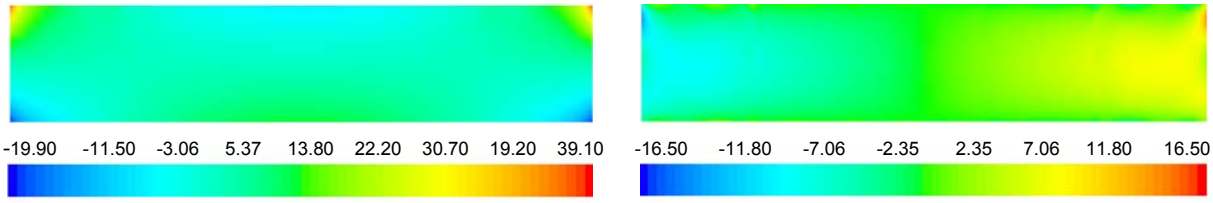

(a) $\tilde{\sigma}_{yy}$ (MPa) (b) $\tilde{\sigma}_{yz}$ (MPa)

Figure 3 – Example 1: effective stress distribution on nonlinear regime for t_γ= 0.75MPa by the damage model of [Mazars, 1984] (plane x=1.0m).

Damage model by [Comi and Perego, 2001]	$\tilde{\sigma}_{yy}$ (MPa)	$\tilde{\sigma}_{yz}$ (MPa)
	[-17.70 ; 54.10]	[-16.50 ; 16.50]

Table 1 - Example 1: summary of the effective stresses on damage model by [Comi and Perego, 2001] for t_γ=0.75MPa (plane x=1.0m).

As expected, the damaging process begins at the fixed sections of the beam and the material degradation develops from the top fibers of the cross section due to the high stress $\tilde{\sigma}_{yy}$. Moreover, to an advanced loading state the important tensile strains at the bottom fibers of mid-spam zone explain the arising of cracking at that zone. The damage diagrams obtained by the models of [Comi and Perego, 2001] and [Mazars, 1984] support the previous statement and enable the comparison of damage on the sections where there are high tensile strains. These are presented in Figures (4) and (5), respectively, and along with the deformed configuration.

Both models reproduce the cracking process, namely the beginning of cracking process at the fixed sections and the appearance of damage at the mid-spam zone. However, for the model of [Comi and Perego, 2001] the initial damage occurs for a load equal to 0.3MPa, while it is equal to 0.26MPa for the model of [Mazars, 1984]. Besides, at an intermediate load state, the damage value in the last one is greater than in the first one. Despite the damage models present a similar maximum damage value

at fixed sections, the model of [Mazars, 1984] leads to a larger damaged area at those zones and at the mid-spam zone, as illustrated in Figures (4.a.2) and (5.a.2).

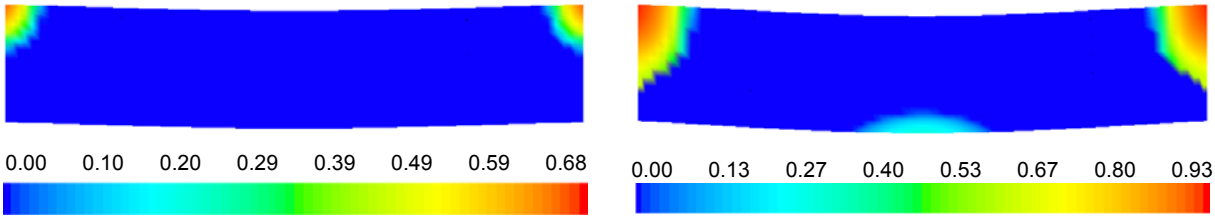

(a.1) damage (t_γ= 0.50MPa) (a.2) damage (t_γ= 0.75MPa)

Figure 4– Example 1: Evolution of damage by the model of [Comi and Perego, 2001] (deformed configuration with a scale factor of 100, plane x=1.0m).

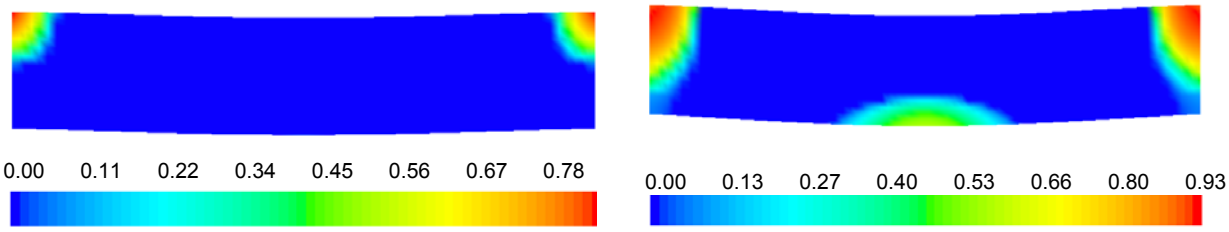

(a.1) damage (t_γ= 0.50MPa) (a.2) damage (t_γ= 0.75MPa)

Figure 5– Example 1: Evolution of damage by the model of [Mazars, 1984] (deformed configuration with a scale factor of 100, plane x=1.0m).

6.2 Example 2: L-shaped structure

In this example, a three-dimensional structure geometrically similar to an *L* is considered with a full moment connection on the basis and an uniform prescribed displacement at the *L*'s tip, as illustrated in Figure (6). A mesh with three finite elements is adopted and each one corresponds to a cube characterized by an edge's length equal to 1m. The degrees of the aproximation functions are $n_{S_v} = 5$, $n_{U_v} = 4$ and $n_{U_\gamma} = 3$, which corresponds to 5717 degrees of freedom. The numerical results are obtained by considering a mesh of (20x20x20) Lobatto integration points.

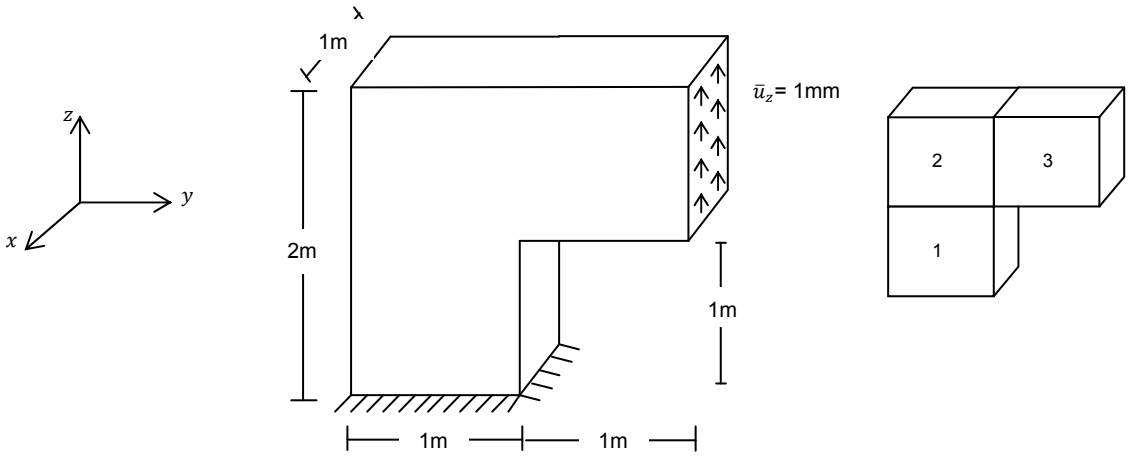

Figure 6 – Example 1: Definition of the geometry, the load case and the finite elements mesh.

This structure is characterized by a singularity where occurs a strong concentration of tensile strains that sets the cracking process in the inward corner. It is possible to confirm that localization checking the stress distribution in linear regime. The diagram that represents the stress σ_{zz} (Figure (7.c)) also presents high tensile stresses in the adjacent zone spreading to the fixed face. Thus, both damage models must reproduce the beginning of the cracking process in the singularity and its evolution to the fixed section.

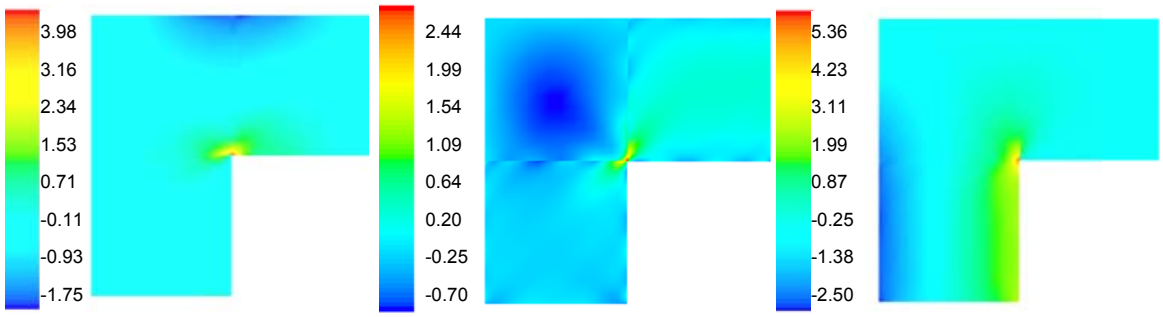

(a) σ_{yy} (MPa) (b) σ_{yz} (MPa) (c) σ_{zz} (MPa)

Figure 7 – Example 2: stress distribution on linear regime for $\bar{u}_z$=0.50mm (plane x=0.5m).

The discrepancy between the distributions of effective stress obtained by these two damage models, mainly at the diagram $\tilde{\sigma}_{zz}$, makes important the presentation of that diagram for both models.

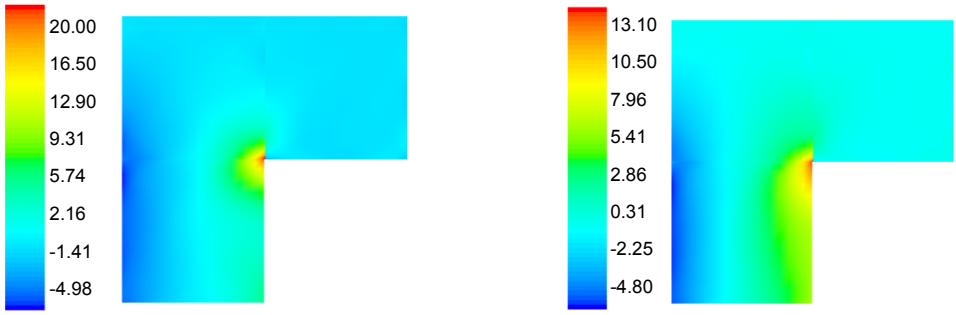

(a) $\tilde{\sigma}_{zz}$ (MPa) – [Comi and Perego, 2001] (b) $\tilde{\sigma}_{zz}$ (MPa) – [Mazars, 1984]

Figure 8 – Example 2: effective stress $\tilde{\sigma}_{zz}$ distribution for $\bar{u}_z$=1.00mm by the models of [Comi and Perego, 2001] and [Mazars, 1984] (plane x=1.0m).

The effective stresses reproduced by the damage model of [Comi and Perego, 2001] are greater than those obtained on the model of [Mazars, 1984]. Moreover, the first one presents only high stress $\tilde{\sigma}_{zz}$ at the singular zone (Figure 8.a), while the other model also shows important stress in the adjacent zone and near the basis (Figure 8.b). Thus, the evolution of damage is a little different, as illustrated on the Figures (9) and (10).

In both models, the initial microcracks arise at the singularity of the structure for a displacement equal to 0.53mm. According to the damage model of [Comi and Perego, 2001], the development of cracking occurs mainly on that zone and therefore it is there that the coalescence of microcracks occurs (Figure 9). Despite the model of [Mazars, 1984] presents an advanced degradation state of the material on the

singularity, but with a lowest damage value, it also reproduces the existence of cracking down to the basis (Figure 10). However, the using of these damage models enables to model the cracking process at the zone of the structure where the more important tensile stress occurs.

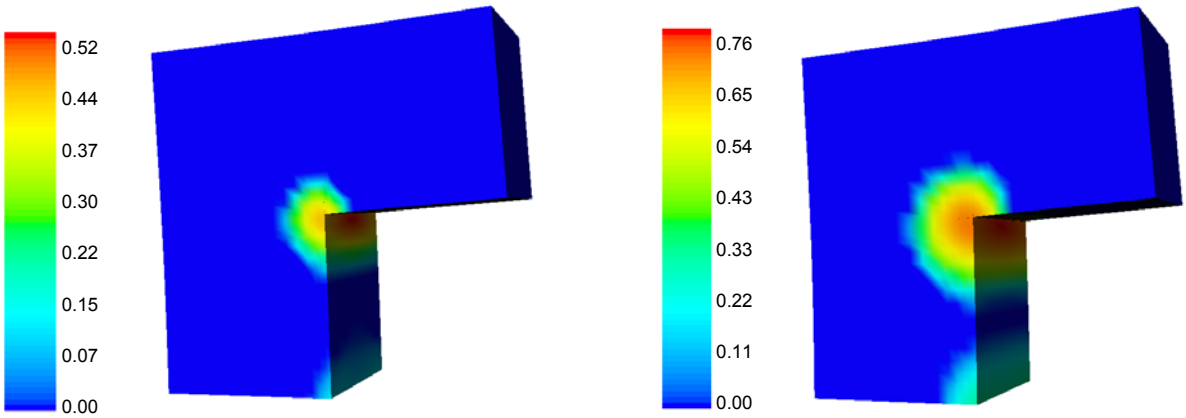

(a) Damage ($\bar{u}_z$=0.75mm) (b) Damage ($\bar{u}_z$=1.00mm)

Figure 9– Example 2: Evolution of damage by the model of [Comi and Perego, 2001] (deformed configuration with a scale factor of 100, plane x=1.0m).

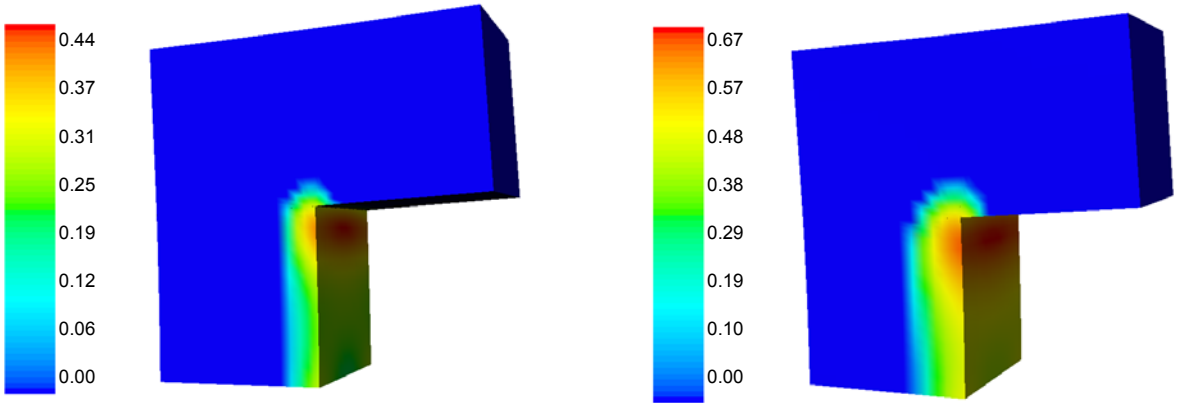

(a) Damage ($\bar{u}_z$=0.75mm) (b) Damage ($\bar{u}_z$=1.00mm)

Figure 10– Example 2: Evolution of damage by the model of [Mazars, 1984] (deformed configuration with a scale factor of 100, plane x=1.0m).

7. Conclusions and Future Developments

An accurate modeling of the mechanic concrete behavior must be adopted on the design of structures, specially the cracking phenomena. The main goal of this communication is to document the use of a hybrid-mixed stress model which embodying Continuum Damage Mechanics to the physically non-linear analysis of the behavior of concrete three-dimensional structures.

In these models, a solution with an acceptable quality leads to a high number of degrees of freedom. The use of Orthonormal Legendre polynomials as approximations functions enables to obtain a high sparsity of the governing system, which makes the model more competitive. However, it is necessary

to establish an appropriate relation between the degrees of the approximation functions to avoid spurious modes and to ensure an adequate conditioning for the governing system.

The damage models considered to attain the main objective of this communication have some limitations. The damage model of [Mazars, 1984] is suitable to concrete structures which collapse mechanism is associated with cracking phenomena due to tensile or compression strains, while the damage model presented by [Comi e Perego, 2001] is only suitable in the first situation. Both models must consider a characteristic length that assures the existence of two/three control points on the Fracture Process Zone. However, if the degradation state of the material reaches a certain level, a discrete crack model, which considers the discontinuity of the displacement field, must be introduced in order to enable a more realistic description of the concrete behaviour.

In this communication, only structures with a regular geometry were analysed. Nevertheless, the model can be extended to general geometries using a simple mapping technique, but *expensive* numerical integration schemes have to be adopted. It is also important to explore the improvement of the numerical performance through the implementation of a parallel processing and adaptive algorithms based on non-uniform refinement procedures.

8. Acknowledgments

This work has been supported by FCT and “FEDER” through the projects PTDC/ECM/71519/2006.

9. References

[Almeida, 1991] Almeida, J. P. M. (1991). *Modelos de elementos finitos para a análise elastoplástica.* Ph.D. thesis, Technical University of Lisbon, Lisbon;

[Bazant, 1992], Bazant, Z. P. (1992). *Fracture Mechanics of Concrete Structures.* Elsevier Applied Science, London.

[Comi and Perego, 2001] Comi, C. e Perego, U. (2001). Nonlocal aspects of nonlocal damage analyses of concrete structures. *European Journal of Finite Elements*, 10:227-242.

[Lemaitre, 1992] Lemaitre, J. (1992). *A course on damage mechanics.* Springer-Verlag, first edition;.

[Lemaitre e Chaboche, 1988] Lemaitre, J. e Chaboche, J.-L. (1985). *Mécanique des matériaux solides.* Dunod, 2ª edition.

[Mazars, 1984] Mazars, J. (1984). *Application de la mécanique de l’endommagement au comportement non lineaire et à la rupture du béton de structure.* Ph. D. thesis, Université Paris 6, Paris.

[Mazars et al., 1991] Mazars, J., Pijaudier-Cabot, G., e Saouridis, C. (1991). Size effect and continuous damage in cementitious materials. *International Journal of Fracture,* 51:159-173.

[Pereira e Freitas, 2000] Pereira, E. M. B. R. e Freitas, J. A. T. (2000). *Numerical implementation of a hybrid-mixed finite element model for reissner-mindlin plates.* Computers & Structures, 74: 323-334.~

[Perego, 1990] Perego, M. (1990). *Dannegiamento dei materiali lapidei: leggi costitutive, analisis per elementi finiti ed apllicazioni. Ph.D. thesis*, Politecnic of Milano.

[Pijaudier-Cabot et al., 1994] Pijaudier-Cabot, G., Dubé, J.F., la Borderie, Ch. E Bodé, L. (1994). Damage models for concrete in transient dynamics. Em Bazant, Z. P., Bittnar, Z., Jirásek, M. e Mazars, J., editors, *Fracture and Damage in Quasi-brittle Structures: Experiment, Modeling and Computer Analysis,* pages 201-215. E and FN Spon, London.

[Silva, 2006] Silva, M. C. O. M. (2006). *Modelos de Dano em Elementos Finitos Híbridos e Mistos*. Ph.D. thesis, Technical University of Lisbon, Lisbon;

[Timoshenko and Goodier, 1970] Timoshenko, S. P. e Goodier, J. N. (1970). *Theory of elasticity.* McGraw-Hill, 3ª edition;

[Zienkiewicz and Taylor, 1991] Zienkiewicz, O. C. e Taylor, R. L. (1991b). *The finit element method, Vol.2 – Solid and Fluid Mechanics, Dynamics and Non-Linearity.* McGraw-Hill, 4ª edition;